Spectral Properties and Transport Mechanisms of Partially Chaotic Bounded Flows in the Presence of Diffusion

M. Giona,* A. Adrover, S. Cerbelli, and V. Vitacolonna

Dipartimento di Ingegneria Chimica, Università di Roma "La Sapienza," via Eudossiana 18, 00184 Roma, Italy

(Received 25 July 2003; published 18 March 2004)

The spectral properties of the Poincaré operator associated with the advection-diffusion equation for partially chaotic periodic flows defined in bounded domains are analyzed in this Letter. For vanishingly small diffusivities (i.e., for the Peclet number tending to infinity) the dominant eigenvalue Λ exhibits the scaling $\Lambda \sim \mathrm{Pe}^{-\alpha}$, where the exponent $\alpha \in (0, 1)$ depends on the global property of the flow (shape, geometry, and symmetry of quasiperiodic islands). The value of the exponent α is an indicator of qualitatively different transport mechanisms and depends on the localization properties of the corresponding eigenfunctions.

DOI: 10.1103/PhysRevLett.92.114101 PACS numbers: 05.45.–a, 47.54.+r, 83.50.Xa, 47.52.+j

The understanding of transport processes in chaotic flows is a central issue in many fields of applied and theoretical sciences [1]. By restricting our attention to scalar fields and incompressible flows, the core of the problem is the coupling between advection and diffusion, described by the equation

$$\frac{\partial \phi}{\partial t} + \mathbf{v} \cdot \nabla \phi = \frac{1}{\mathrm{Pe}} \nabla^2 \phi, \tag{1}$$

where $\mathbf{v}$ is the velocity field ($\nabla \cdot \mathbf{v} = 0$) and Pe is the Peclet number, representing the ratio of the characteristic diffusion time scale to that of advection. The implications of Eq. (1) go beyond fluid dynamics and mixing theory, since (i) the advection-diffusion operator provides the simplest example of linear non-self-adjoint operator, ubiquitous in physical sciences, the qualitative properties of which are not fully understood, (ii) Eq. (1) is one to one with the evolution of dynamical systems driven by noise, expressed as a Wiener process [2], and (iii) the correspondence between Eq. (1) and the kinematic equations $\dot{\mathbf{x}} = \mathbf{v}(\mathbf{x}, t)$ provides useful hints for approaching the quantum-to-classical transition [3], by making use of Wigner functions and the quantum Liouville equation, and vice versa.

Results on the advection-diffusion dynamics have been obtained by applying several different approaches [4–12]. These results refer to both bounded and unbounded flow geometries, but significant physical and mathematical differences occur between these situations.

Throughout this Letter, we focus exclusively on bounded partially chaotic flows, which give rise in the diffusionless Poincaré section to regions of quasiperiodic motion intertwined by regions of chaotic kinematics. This is the most suitable setting for analyzing the interplay between stretching and folding, characterizing advection and diffusion (i.e., the dispersion properties). The aim of this Letter is to provide a fairly comprehensive analysis of the typical qualitative properties of dispersion and to highlight how these properties are related to different transport mechanisms.

Owing to the linearity of Eq. (1), and to the boundedness of the domain, spectral (i.e., eigenvalue or eigenfunction) analysis of the advection-diffusion operator (or of the associated Poincaré operator in the case of time-periodic flows) provides a complete characterization of dispersion properties.

As a model of partially chaotic flows, the time-periodic sine flow (TPSF), which has been widely referred to in previous studies [13], is considered. The TPSF system is defined as the periodic sequence of two steady sinusoidal flows, $\mathbf{v}_1(\mathbf{x}) = (v_{1,x}, v_{1,y}) = (\sin(2\pi y), 0)$, and $\mathbf{v}_2(\mathbf{x}) = (0, \sin(2\pi x))$, acting alternately for a time $T/2$ on points $\mathbf{x} = (x, y)$ of the unit square $\mathcal{I}^2 = [0, 1) \times [0, 1)$ with opposite edges identified. Figures 1(a)–1(d) show the Poincaré section of the TPSF for several values of the period T, corresponding to partially chaotic flows possessing different sizes and symmetries of the quasiperiodic islands.

By expanding the scalar field ϕ with respect to the eigenbasis of the Laplacian operator $\{e^{2\pi i(rx+sy)}\}_{r,s=-\infty}^{\infty}$, $\phi(\mathbf{x}, t) = \sum_{r,s} \phi_{r,s}(t) e^{2\pi i(rx+sy)}$, the evolution equation for the Fourier coefficients $\phi_{r,s}(t)$ reads

$$\frac{d\phi_{r,s}}{dt} = -\frac{4\pi^2(r^2 + s^2)}{\mathrm{Pe}} \phi_{r,s} - \pi r(\phi_{r,s-1} - \phi_{r,s+1}) \tag{2}$$

for $nT \le t \le (2n + 1)T/2$, $n = 0, 1, \ldots$. The evolution equation for the second half period is obtained by interchanging the subscripts r and s.

In the case of the TPSF, the Poincaré operator $\mathcal{P}$ mapping $\phi^{(n)}(\mathbf{x}) = \phi(\mathbf{x}, nT)$ over a period T, $\phi^{(n+1)}(\mathbf{x}) = \mathcal{P}[\phi^{(n)}(\mathbf{x})]$ is given by $\mathcal{P}[\phi] = e^{\mathcal{L}_2 T/2} \circ e^{\mathcal{L}_1 T/2}$, where $\mathcal{L}_i = -\mathbf{v}_i(\mathbf{x}) \cdot \nabla + \mathrm{Pe}^{-1}\nabla^2$, $i = 1, 2$. The operator $\mathcal{P}$ acts on the functional space $L^2_{\mathrm{per}}(\mathcal{I}^2)$ of square-summable periodic functions in $\mathcal{I}^2$. $\mathcal{P}$ admits the constant function as a nondegenerate eigenfunction associated with the

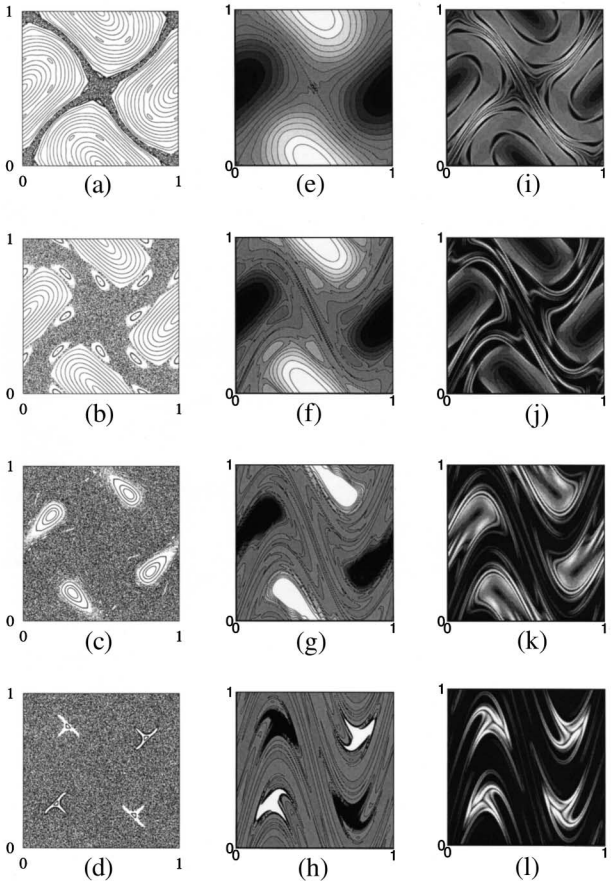

FIG. 1. First column: Poincaré section of the TPSF. (a) $T = 0.4$; (b) $T = 0.56$; (c) $T = 0.8$; (d) $T = 1.18$. Second column: contour plot of the dominant eigenfunction. Dark and light correspond to negative and positive values, respectively. (e) $T = 0.4$, $\mathrm{Pe} = 10^5$, $N = 150$; (f) $T = 0.56$, $\mathrm{Pe} = 10^5$, $N = 150$; (g) $T = 0.8$, $\mathrm{Pe} = 4 \times 10^4$, $N = 140$; (h) $T = 1.18$, $\mathrm{Pe} = 4 \times 10^4$, $N = 140$. Third column: contour plot of the gradient norm of the dominant eigenfunction. Dark and light correspond to small and high values of $|\nabla\phi(\mathbf{x})|$, respectively. (i) $T = 0.4$, $\mathrm{Pe} = 10^5$, $N = 150$; (j) $T = 0.56$; $\mathrm{Pe} = 10^5$, $N = 150$; (k) $T = 0.8$; $\mathrm{Pe} = 4 \times 10^4$, $N = 140$; (l) $T = 1.18$, $\mathrm{Pe} = 4 \times 10^4$, $N = 140$.

eigenvalue 1. In the analysis of homogenization and dispersion, $\mathcal{P}$ can be defined in the space $\dot{L}^2_{\mathrm{per}}(I)$ of the functions belonging to $L^2_{\mathrm{per}}(I)$ and possessing zero mean, i.e., $\int_{I^2} \phi(\mathbf{x}) d\mathbf{x} = 0$. Obviously, $\dot{L}^2_{\mathrm{per}}(I)$ is an invariant subspace for $\mathcal{P}$. Spectral analysis of the Poincaré operator is performed by considering its truncation $\mathcal{P}_N$ over the finite-dimensional subspace L_N spanned by $\{e^{2\pi i(rx+sy)}\}_{r,s=-N}^{N}$. The generalized eigenspectrum of P_N forms a basis for L_N, and the operator $\mathcal{P}$ is compact. Owing to the compactness of $\mathcal{P}$, the eigenvalues $\{\mu_k\}$ of $\mathcal{P}$ can be ordered in a nonincreasing way, with respect to their moduli. The greatest eigenvalue, say μ_1, dominates the exponential scaling of the norm of $\phi(\mathbf{x}, t)$, starting from generic initial conditions. In a time-continuous frame we refer to the dominant eigenvalue Λ, defined as $\Lambda = -\log|\mu_1|/T$. This means that for generic initial conditions, the square-integral norm of $\phi(\mathbf{x}, t)$ scales as $\|\phi\|_{L^2}(t) \sim \exp(-\Lambda t)$ for $t \to \infty$.

The eigenvalue or eigenfunction spectrum of P_N is obtained by applying the QZ algorithm, and the power method in the case of real dominant eigenvalues. The truncation order N is chosen, case by case, so as to ensure the accuracy of the corresponding eigenvalues or eigenfunctions. While for $\mathrm{Pe} = 10^3$, $N = 60$–70 is fully sufficient, the truncation order N should be larger for higher values of Pe, up to $N = 150$ (corresponding to 150^2 Fourier modes) for $\mathrm{Pe} = 10^5$.

Let us now consider the physical properties of dispersion, by analyzing the spectral structure of the Poincaré operator. A first qualitative property of partially chaotic flows is that the eigenvalue spectrum can be partitioned into several distinct subsets (branches) each of which being characterized by a different scaling behavior of the eigenvalues with the Peclet number. More specifically, two eigenvalue branches exist which are referred to as the C(for cosine) and the S branch (for sine). Their respective eigenfunctions $\psi_{r,s}$ are characterized by the property $\mathrm{Im}[\psi_{r,s}] = 0$ for the C branch and $\mathrm{Re}[\psi_{r,s}] = 0$ for the S branch. This naturally follows from the fact that the coefficient matrix for the Fourier coefficients [see Eq. (2)] possesses real entries. The two spectral branches are shown in Figs. 2(b) and 2(b) for the TPSF at $T = 0.4$ and $T = 0.8$, respectively. In these figures $\lambda_n = -\log|\mu_n|/T$. The dominant eigenvalue of each branch follows a power-law scaling with the Peclet number

$$\lambda_n \sim \mathrm{Pe}^{-\alpha}, \tag{3}$$

and the exponents characterizing the C and the S branch are in general different. When $T = 0.4$, the dominant eigenvalue belongs to the C branch, is real, and follows a diffusional scaling $\lambda_n \sim \mathrm{Pe}^{-1}$, while the dominant eigenvalue of the S branch is complex and behaves as $\lambda_n \sim \mathrm{Pe}^{-1/2}$. The latter scaling (i.e., $\alpha = 1/2$) also characterizes the behavior of autonomous flows: it has been justified in [14] and named by Fannjiang and Papanicolau [12] *convection-enhanced diffusion*. For $T = 0.8$ [Fig. 2(b)], the dominant eigenvalue in the range $\mathrm{Pe} \in (10^2, 10^5)$ belongs to the C branch and follows Eq. (3) with $\alpha = 0.745$. Conversely, the S branch possesses a dominant eigenvalue that scales diffusively (i.e., $\alpha = 1$). However, as can be extrapolated from the data depicted in Fig. 2(b), for larger Peclet values ($\mathrm{Pe} > 10^6$) a crossing between the two eigenvalue branches will occur, and for such high Peclet values the dominant eigenvalue will eventually scale diffusively. A comprehensive review of the dominant-eigenvalue scaling for the TPSF is depicted in Fig. 3, for several values of T in the range (0.4, 2.0). While the power-law scaling Eq. (3) is always fulfilled, the value of the exponent α depends on the flow protocol. The case $\alpha = 0$ occurs for $T = 1.6$ (curve e) and characterizes globally chaotic conditions, as discussed in [11]. For $T = 0.56$ [curve b; see also Fig. 1(b)] $\alpha = 0.865$, while the case $T = 1.18$ [curve d; see also Fig. 1(d)] shows the value

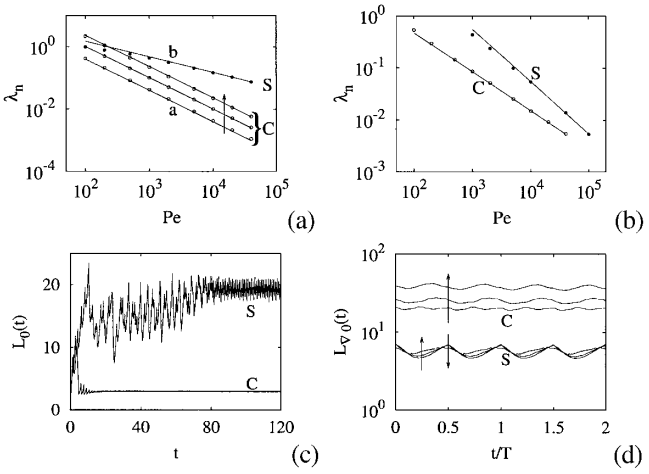

FIG. 2. (a) Dominant eigenvalues of the C and S branch vs Pe at $T = 0.4$. Dots (○) refer to the C branch: the first, second, and third eigenvalues (see the arrow) are depicted. Dots (●) refer to the S branch. Curve (a) represents $\lambda_n = 4\pi^2/\mathrm{Pe}$, curve ($b$) $\lambda_n = A/\sqrt{\mathrm{Pe}}$. (b) Dominant eigenvalues for the two spectral branches (C and S) at $T = 0.8$ vs Pe. The solid lines represent the scalings $\lambda_n \sim \mathrm{Pe}^{-\alpha}$ (C branch) with $\alpha = 0.745$, and $\lambda_n = \sim 1/\mathrm{Pe}$ (S branch), respectively. (c) Reaction interface length $L_0(t)$ vs time t of the solution $\phi(\mathbf{x}, t)$ of Eq. (1) at $T = 0.4$, $\mathrm{Pe} = 5 \times 10^3$, starting from $\phi(\mathbf{x}, 0) = \cos(2\pi x)$ (label C), and from $\phi(\mathbf{x}, 0) = \sin(2\pi x)$ (label S). (d) Length $L_{\nabla 0}$ of the zero-level set of the gradient norm $G(\mathbf{x}) = |\nabla\psi(\mathbf{x})| - \langle|\nabla\psi(\mathbf{x})|\rangle$ of the dominant eigenfunction vs t/T for $T = 0.8$. The C bundle refers to the C branch, the S bundle to the S branch. The arrows indicate increasing values of $\mathrm{Pe} = 5 \times 10^3$, 10^4, 4×10^4.

$\alpha = 0.55$. An interesting case occurs for $T = 2.0$. The Poincaré section of the stroboscopic kinematics is seemingly globally chaotic. A more accurate analysis reveals the existence of small islands that include the two elliptic points located at (1/4, 1/4) and (3/4, 3/4). The scaling of the dominant eigenvalue of the advection-diffusion Poincaré operator is very sensitive to the lack of globally chaotic conditions and is characterized by the value $\alpha = 0.37$, which is different from the value $\alpha = 0$ obtained for global chaos. The exponent α is not a monotonic function

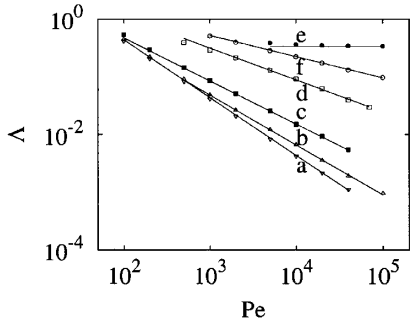

FIG. 3. Dominant eigenvalue Λ vs Pe for the TPSF system. The dominant eigenvalue follows the scaling Eq. (3). (a) $T = 0.4$, $\alpha = 1.0$; (b) $T = 0.56$, $\alpha = 0.865$; (c) $T = 0.8$, $\alpha = 0.745$; (d) $T = 1.18$, $\alpha = 0.55$; (e) $T = 1.6$, $\alpha = 0.0$; (f) $T = 2.0$, $\alpha = 0.37$.

of T. For example, at $T = 0.8$, the dominant exponent for large Pe becomes $\alpha = 1$. Spectral results indicate that the exponent α may be different from 1 for arbitrarily large Pe values. A typical case is represented by $T = 1.18$ for which both the C and the S branches follow an identical power-law scaling, characterized by the exponent $\alpha = 0.55$. The differences between the dominant solutions of the two branches are related to the symmetries of the corresponding eigenfunctions. The values of the exponent α reported above refer to the asymptotic scaling of the dominant eigenvalue for large Pe. The departure from the diffusive scaling $\alpha = 1$ is the fingerprint of an emerging and effective, if nontrivial, coupling between advection and diffusion.

An open question is what determines the occurrence of multiple spectral branches and the values of α. The "multibranch" phenomenon occurs for partially chaotic flows and for two-dimensional autonomous flows [11] but is absent in pure diffusion in the presence of a constant velocity field, and for globally chaotic flows [11]. It is reasonable to argue that the presence of multiple spectral branches is a consequence of the lack of global ergodicity in the kinematic equations of motions $\dot{\mathbf{x}} = \mathbf{v}(\mathbf{x}, t)$. In fact, autonomous and partially chaotic flows are not globally ergodic (since the invariant Lebesgue measure on $\mathcal{I}^2$ is not ergodic), while globally chaotic flows possess this property.

It is more difficult to give a simple and intuitive answer for the factors determining the values of the exponent α. A definitive answer can be obtained for simple two-dimensional autonomous flows $\mathbf{v}(\mathbf{x}) = [0, v_y(x)]$, such as the autonomous sine flow (and extended qualitatively to generic two-dimensional autonomous flows in bounded domains). For these flows, the value $\alpha = 1/2$ is the consequence of the local quadratic behavior of the velocity $v_y(x)$ near the local maxima or minima [15]. For partially chaotic flows, we may argue that the values of α are determined by the global dynamic properties (expressed by structure of the kinematic Poincaré section). This observation is suggested by the structure of the eigenfunctions, which closely mimic the kinematic Poincaré sections for $\mathrm{Pe} \to \infty$. This observation can be looked at the other way around: the spectral analysis of the linear advection-diffusion equation (1) for $\mathrm{Pe} \to \infty$ may be an alternative way for addressing global dynamic properties of the finite-dimensional nonintegrable nonlinear system $\dot{\mathbf{x}} = \mathbf{v}(\mathbf{x}, t)$ (such as the occurrence of quasiperiodic or chaotic regions) without performing explicit numerical simulations of it.

The different values of the scaling exponent α are indicative of the occurrence of different transport mechanisms. In general, the dominant eigenfunction in partially chaotic flows is "localized" for large Pe within the quasiperiodic islands; see Figs. 1(e)–1(h). This is particularly evident from the contour plot of the dominant eigenfunction at $T = 0.56$, $\mathrm{Pe} = 10^5$ [Fig. 1(f)], which is closely similar to the archipelagolike structure of smaller

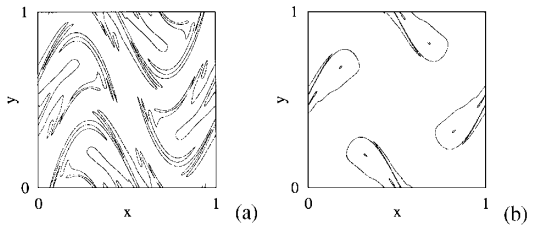

FIG. 4. Zero-level set for the rescaled gradient norm $G(\mathbf{x})$ associated with the dominant eigenfunctions of the TPSF at $T = 0.8$, $\mathrm{Pe} = 10^4$ ($N = 80$). (a) C branch. (b) S branch.

islets, characterizing the Poincaré section of this flow [Fig. 1(b)]. However, a strict eigenfunction localization within the quasiperiodic islands occurs exclusively in the cases in which the eigenvalue branch follows a diffusional scaling (i.e., $\alpha = 1$). In this case, the influence of chaotic advection is negligible, and for $\mathrm{Pe} \to \infty$, the support of the eigenfunctions approaches the structure of the quasiperiodic islands. This phenomenon occurs for the dominant-eigenvalue branch at $T = 0.4$ and for the S branch at $T = 0.8$ and can be fully appreciated by considering other geometric indicators. Figure 2 shows the length $L_0(t)$ of the reaction interface [10], i.e., the zero-level set of the function $\phi(\mathbf{x}, t)$ solution of Eq. (1), for $T = 0.4$, $\mathrm{Pe} = 5 \times 10^3$ for two different initial conditions: a cosine function (exciting the C branch) and a sine function (exciting the S branch). For the C-branch solution, approaching the dominant diffusive eigenfunction, the reaction interface saturates asymptotically towards a constant low value which for $\mathrm{Pe} \to \infty$ converges towards the perimeter length of the separatrices of the two main quasiperiodic islands. An analogous feature can be observed in Fig. 2(d), which depicts for $T = 0.8$ the length $L_{\nabla 0}$ of the zero-level set of the rescaled gradient norm $G(\mathbf{x}) = |\nabla\psi(\mathbf{x})| - \langle|\nabla\psi|\rangle$, ($\langle|\nabla\psi|\rangle = \int_{I^2}[(\partial_x\psi)^2 + (\partial_y\psi)^2]^{1/2} d\mathbf{x}$ of the dominant eigenfunctions of the two branches. For the diffusional branch (S branch), the length $L_{\nabla 0}$ does not practically change with Pe, since the zero-level set of $G(\mathbf{x})$ approaches the external perimeter of the quasiperiodic islands [Fig. 4(b)]. Conversely, $L_{\nabla 0}$ grows monotonically with Pe for the C branch. This implies that the latter case is characterized by a geometrically convoluted boundary layer, deeply located within the chaotic region, and whose perimeter length diverges from $\mathrm{Pe} \to \infty$. The latter phenomenon is clearly evident from the contour plots of the gradient norm $|\nabla\psi|$ for $T = 0.56$, 0.8, and 1.18 [Figs. 1(j)–1(l)], and for the zero-level set of the eigenfunction [Fig. 4(a)] at $T = 0.8$. The boundary layer on which gradients are localized resembles a system of flamelets penetrating the chaotic region. This boundary layer is responsible for the occurrence of an exponent α less than 1, and for this reason the transport mechanism associated with this situation can be referred to as *interisland chaos-mediated diffusion:* the concentration field is mainly localized within the regular islands, but homogeneization is controlled by the leaking of material entity from the islands into the chaotic region and therein rapidly dispersed by chaotic advection.

The results obtained in this Letter can be summarized as follows: (i) the occurrence of an exponent α less than 1, and the spectral multibranch behavior in partial chaotic flows seems to be a consequence of the lack of global ergodicity, and depends upon the complex structure of the kinematic Poincaré sections; (ii) spectral heterogeneity (occurrence of different eigenvalue branches) is related to the coexistence of different transport mechanisms (diffusional or chaos-mediated transport) within one and the same flow; (iii) the localization properties of the eigenfunctions depend on the transport mechanism: in particular, diffusional ($\alpha = 1$) and chaos-mediated eigenfunctions behave differently.

*To whom correspondence should be addressed.

[1] S. Childress and A. D. Gilbert, *Stretch, Twist, Fold: The Fast Dynamo* (Springer-Verlag, Berlin, 1995).
[2] S. Chandrasekhar, Rev. Mod. Phys. **15**, 1 (1943); A. Lasota and M. C. Mackey, *Chaos, Fractals and Noise* (Springer-Verlag, New York, 1994).
[3] T. F. Jordan and E. C. G. Sundaram, Rev. Mod. Phys. **33**, 515 (1961); J. E. Moyal, Proc. Cambridge Philos. Soc. **45**, 99 (1949); T. Bhattacharya, S. Habib, and K. Jacobs, Phys. Rev. Lett. **85**, 4852 (2000).
[4] P. Castiglione, A. Mazzino, A. P. Muratore-Gianneschi, and A. Vulpiani, Physica (Amsterdam) **134D**, 75 (1999).
[5] T. M. Antonsen, Jr., Z. Frank Fan, and E. Ott, Phys. Rev. Lett. **75**, 1751 (1995); T. M. Antonsen, Z. Fan, E. Ott, and E. Garcia-Lopez, Phys. Fluids **8**, 3094 (1996); A. Wonhas and J. C. Vassilicos, Phys. Rev. E **66**, 051205 (2002).
[6] V. Rom-Kedar and A. C. Poje, Phys. Fluids **11**, 2044 (1999).
[7] I. Klapper, Phys. Fluids A **4**, 861 (1992).
[8] V. Toussaint, P. Carriere, J. Scott, and J.-N. Gence, Phys. Fluids **12**, 2834 (2000).
[9] R. Reigada, F. Sagues, I. M. Sokolov, J. M. Sancho, and A. Blumen, Phys. Rev. Lett. **78**, 741 (1997); Z. Neufeld, C. Lopez, and P. H. Haynes, Phys. Rev. Lett. **82**, 2602 (1999).
[10] M. Giona, S. Cerbelli, and A. Adrover, Phys. Rev. Lett. **88**, 024501 (2002).
[11] A. Adrover, S. Cerbelli, and M. Giona, J. Phys. Chem. A **105**, 4908 (2001); S. Cerbelli, A. Adrover, and M. Giona, Phys. Lett. A **312**, 355 (2003).
[12] A. Fannjiang and G. Papanicolau, SIAM J. Appl. Math. **54**, 333 (1994); **62**, 129 (2001).
[13] M. Liu, F. Muzzio, and R. L. Peskin, Chaos Solitons Fractals **4**, 869 (1994); M. M. Alvarez, F. J. Muzzio, S. Cerbelli, A. Adrover, and M. Giona, Phys. Rev. Lett. **81**, 3395 (1998).
[14] S. Childress and A. M. Soward, J. Fluid Mech. **205**, 99 (1989).
[15] M. Giona, S. Cerbelli, and V. Vitacolonna, "Universality and Imaginary Potentials in Advection-Diffusion Equations in Closed Flows" (unpublished).